EPJ Web of Conferences **312**, 02011 (2024) https://doi.org/10.1051/epjconf/202431202011
FPCP 2024

Quantum decoherence and CP violation at Protvino to ORCA experiment

Chinmay Bera[1,*] and *Deepthi* K N[1,**]

[1]Department of Physics, École Centrale School of Engineering - Mahindra University, Hyderabad, Telangana, 500043, India

Abstract. In this work, we study the impact of the environmental decoherence at Protvino to ORCA (P2O) experiment which has a substantial baseline of 2595 kilometres. We simulate this experiment assuming different phenomenological models and considering energy dependency of decoherence parameter, $\gamma \propto E_\nu^n$. Here, E_ν is the neutrino energy and $n = 0, \pm 1, \pm 2$. We estimate the sensitivity of P2O experiment to obtain the upper bounds on γ parameters in each of these cases. Additionally, we use these bounds to illustrate the effect of environmental decoherence on mass hierarchy (MH) and CP violation (CPV) sensitivity of this experiment.

We have noted that P2O poses the strong bound on $\gamma \leq 1.89 \times 10^{-24}\ GeV$ (90% CL) for the case of $n = 0$. Moreover, we observed that while the MH sensitivity has not changed significantly in all the cases, CP violation sensitivity increased above the standard case for all true values of δ_{CP}.

1 Introduction

A new era in neutrino physics research has begun after the discovery and experimental verification of neutrino oscillations. In this captivating phenomenon neutrinos change their identities during propagation, which is governed by the coherent superposition of massive neutrinos. However, the small mass splittings among the massive neutrinos maintain the coherence over the long distances and the weak interaction of neutrinos with matter lead them to be stable in a coherent state.

In the standard neutrino propagation we consider neutrino system to be isolated from its environment i.e., it behaves as a closed system. However, in realistic scenario perfect isolation of quantum system from its environment is infeasible. The presence of environmental factors (open quantum system approach), such as matter density gradients, space-time fluctuation at the Planck scale (space-time foam) and other astrophysical conditions can introduce a non-standard effects which alter the coherent evolution of neutrino states and impact their oscillation patterns. This phenomenon is popularly known as environmental decoherence in neutrino oscillations. Note that this is different from the neutrino wave-packet decoherence in which wave packets of neutrino mass states are spatially separated. Our study primarily focuses on the impact of environmentally induced decoherence on the neutrino oscillations.

[*]e-mail: chinmay20pphy014@mahindraunivesity.edu.in
[**]e-mail: nagadeepthi.kuchibhatla@mahindrauniversity.edu.in

There are numerous studies that discuss neutrino oscillations including environmental decoherence. Here we provide some of the interesting references for comprehensive overview of this effect on various ongoing and upcoming neutrino oscillation experiments. The current bounds on γ from different experimental data analyses such as accelerator experiments (MINOS/MINOS+, T2K, NOvA), reactor experiments (KamLAND, Daya Bay, RENO) and atmospheric experiments (IceCube/DeepCore) have been presented in refs. [1–8]. Additionally, after simulating upcoming experiments such as JUNO and DUNE the authors have listed future bounds on γ in refs. [8–10].

As we are entering into the precision era there is a significant opportunity to probe new physics (NP) with high precision upcoming neutrino oscillation experiments. Environmental decoherence is one such NP effect which alters the standard oscillation probabilities by introducing a damping term $e^{-\gamma L}$ (γ is decoherence parameter and L propagation length of neutrinos, termed as baseline) with the interference terms in the oscillation probabilities. Since the damping term depends on L, for a long baseline (L) one could expect observable decoherence effects. In light of this, we decide to choose Protvino to ORCA (P2O) experiment having a substantial baseline of 2595 km in the study of environmental decoherence effect on the neutrino oscillations.

We have explored the intricacies of environmental decoherence on neutrino oscillation for different phenomenological models as given in table-1 and analysed in a model-independent way. We have obtained future bounds on γ considering power law dependencies ($\gamma \propto E^n$ with $n = 0, \pm1, \pm2$). Among all four models mentioned in table-1 we have discussed first two of models in this proceeding (see ref. [11] for detailed discussion of all models).

2 Mathematical background

Neutrino propagation in the framework of open quantum system engendered loss of quantum coherence due to interaction with the stochastic environment. This loss/dissipation due to environmental interaction is introduced using Lindblad master equation which is represented by the density matrix evolution, in the following form [12, 13]

$$\frac{d\rho_m(t)}{dt} = -i\left[H, \rho_m(t)\right] + \mathcal{D}\left[\rho_m(t)\right] \ , \tag{1}$$

where ρ_m is the density matrix of neutrino in the mass basis and H is the Hamiltonian of the neutrino system. The damping term $\mathcal{D}[\rho_m(t)]$ manifests the details of neutrino system and environment interaction. We parameterize $\mathcal{D}[\rho_m(t)]$ impoing some generic properties of density matrix such as complete positivity and preserving trace normalization. Complete positivity condition gives the Lindblad form of the dissipator as [14]

$$\mathcal{D}\left[\rho_m(t)\right] = \frac{1}{2}\sum_{n=1}^{N^2-1}\left\{[\mathcal{V}_n, \rho_m \mathcal{V}_n^\dagger] + [\mathcal{V}_n\rho_m, \mathcal{V}_n^\dagger]\right\} \ , \tag{2}$$

where N is the dimension of the Hilbert space and $\mathcal{V}_n$ are the interaction operators. Further, we impose increase in von Neumann entropy $S = -Tr(\rho_m \ln \rho_m)$ [15, 16] and conservation of average energy $Tr(\rho_m H)$ of the neutrino system and obtain time evolved density matrix [10, 11, 17],

$$\rho_m(t) = \begin{pmatrix} \rho_{11}(0) & \rho_{12}(0)\exp -(\gamma_{21} + i\Delta_{21})^* t & \rho_{13}(0)\exp -(\gamma_{31} + i\Delta_{31})^* t \\ \rho_{21}(0)\exp -(\gamma_{21} + i\Delta_{21}) t & \rho_{22}(0) & \rho_{23}(0)\exp -(\gamma_{32} + i\Delta_{32})^* t \\ \rho_{31}(0)\exp -(\gamma_{31} + i\Delta_{31}) t & \rho_{32}(0)\exp -(\gamma_{32} + i\Delta_{32}) t & \rho_{33}(0) \end{pmatrix}. \tag{3}$$

with

$$\gamma_{jk} = \gamma_{kj} = \frac{1}{2}\sum_{n=1}^{8}(d_{n,j} - d_{n,k})^2 \,, \tag{4}$$

where, $d_{n,j}$, $d_{n,k}$ are the diagonal elements of $\mathcal{V}_n$ operator and j, k take the values $1, 2, 3$.

Since, we are interested in flavor changing phenomenon, conversion of density matrix from mass to flavor basis is obtained by

$$\tilde{\rho}_\alpha = \tilde{U}\,\tilde{\rho}_m\,\tilde{U}^\dagger \,, \tag{5}$$

where $\tilde{U}$ is the matter modified PMNS matrix. The modified mixing parameters due to MSW effect are taken from ref. [18] .

The neutrino transition probability from initial flavor 'ν_α' to final flavor 'ν_β' in terms of density matrix is

$$P_{\alpha\beta}(t) = Tr[\tilde{\rho}_\alpha(t)\tilde{\rho}_\beta(0)] \,. \tag{6}$$

The explicit form of the transition probability assuming ultra-relativistic neutrinos ($t \approx L$) is given by [6, 10, 11]

$$P_{\alpha\beta}(L) = \delta_{\alpha\beta} - 2\sum_{j>k} Re\left(\tilde{U}_{\beta j}\tilde{U}^*_{\alpha j}\tilde{U}_{\alpha k}\tilde{U}^*_{\beta k}\right) + 2\sum_{j>k} Re\left(\tilde{U}_{\beta j}\tilde{U}^*_{\alpha j}\tilde{U}_{\alpha k}\tilde{U}^*_{\beta k}\right)\exp\left(-\gamma_{jk}L\right)\cos\left(\frac{\tilde{\Delta}m^2_{jk}}{2E}L\right)$$
$$+ 2\sum_{j>k} Im\left(\tilde{U}_{\beta j}\tilde{U}^*_{\alpha j}\tilde{U}_{\alpha k}\tilde{U}^*_{\beta k}\right)\exp\left(-\gamma_{jk}L\right)\sin\left(\frac{\tilde{\Delta}m^2_{jk}}{2E}L\right). \tag{7}$$

Here in eq. (7), γ_{jk} appear in the decoherence term $e^{-\gamma_{jk}L}$, which alters oscillation probability. We consider a general *power law* dependency of γ_{jk} on the neutrino energy given by

$$\gamma_{jk}(E_\nu) = \gamma_0\left(\frac{E_\nu}{E_0}\right)^n \,, \tag{8}$$

where, γ_0 is constant, $E_0 = 1$ GeV (reference energy) and $n = 0, \pm1, \pm2$. Different physical origins explain the decoherence phenomena leading to different integral power law dependencies [8]. However, from eq. (8) one can note that for $E_\nu > E_0$, decoherence plays significant role when $n \geq 0$, which could yield better constraints on γ.

Table 1: The decoherence models considered in this work.

Cases	Assumptions on γ_{jk}
Case-I	$\gamma_{21} = \gamma_{31} = \gamma_{32} \neq 0$
Case-II	$\gamma_{21} = \gamma_{31},\ \gamma_{32} = 0$
Case-III	$\gamma_{21} = \gamma_{32},\ \gamma_{31} = 0$
Case-IV	$\gamma_{31} = \gamma_{32},\ \gamma_{21} = 0$

3 Simulation details

We simulate P2O experiment using General Long Baseline Experiment Simulator (GLoBES) software [19, 20]. To simulate P2O experiment we consider the experimental parameters as reported by the P2O collaboration in refs. [21, 22], given in table-2. Considering the standard

Table 2: Experimental parameters are used to simulate P2O experiments.

Baseline	2595 km
Detector mass	8 Mton (Water Cherenkov)
Matter density	3.3 gm/cm^3
Run time	6 years ($3(\nu) + 3(\bar{\nu})$)
Exposure	0.8×10^{20} POT/year for 90kW
Analysis window	2 - 12 GeV
Energy resolution	$\approx 30\%$
Particle identification factor	fig. 99 of ref. [22]
Signal normalization error	5%
Background norm. error	12%
Tilt error	11%

three flavour oscillation picture we have reproduced the event spectra w.r.t the true neutrino energy that has been reported in ref. [21].

In addition, we have incorporated a new oscillation probability engine into GLoBES considering open quantum system formalism to introduce effect of decoherence in neutrino oscillation. Then we have obtained the simulated data for both 90kW (P2O) and 450kW (P2O-upgraded) with 6 years (3 years in ν and 3 years in $\bar{\nu}$ mode) of run. The neutrino oscillation parameters and their fit ranges for this analysis are taken from ref. [23], listed in table-3.

4 Analysis routines

For the statistical analysis, the χ^2 function is calculated using Poisson chi-square function given by

$$\chi^2 = \min_{\alpha_s,\alpha_b} \sum_{\text{channels}} 2 \sum_i \left[N_i^{\text{test}} - N_i^{\text{true}} + N_i^{\text{true}} \log\left(\frac{N_i^{\text{true}}}{N_i^{\text{test}}}\right)\right] + \alpha_s^2 + \alpha_b^2 \,, \tag{9}$$

where, N_i^{test} and N_i^{true} are the number of test and true events (signal + background) in i-th bin, respectively. α_s and α_b are the signal and background normalisation errors treated using the *pull method* [24, 25]. We consider $\nu_\mu \to \nu_e$, $\nu_\mu \to \nu_\mu$ oscillation channels along along with corresponding anti-neutrinos channels in the energy window of 2 to 12 GeV. We marginalize over the full range in δ_{CP}, and 3σ ranges in θ_{23}, $(\Delta m^2_{31})_{NH}$ (NH stands for normal hierarchy) without assuming any priors.

- To constraint γ

$$\Delta\chi^2_\gamma = \chi^2(\gamma(true) = 0, \gamma(test) \neq 0) \tag{10}$$

  and marginalized over θ_{23} and δ_{CP}, $(\Delta m^2_{31})_{NH}$.

- To analyze CP violation

$$\begin{aligned} \Delta\chi^2_0 &= \chi^2_{true}(\delta_{CP}(true), \gamma \neq 0) - \chi^2_{test}(\delta_{CP} = 0, \gamma = 0) \,, \\ \Delta\chi^2_\pi &= \chi^2_{true}(\delta_{CP}(true), \gamma \neq 0) - \chi^2_{test}(\delta_{CP} = \pi, \gamma = 0) \,, \\ \Delta\chi^2_{CPV} &= min[\Delta\chi^2_0, \Delta\chi^2_\pi] \,, \end{aligned} \tag{11}$$

  we marginalized over θ_{23}, $(\Delta m^2_{31})_{NH}$.

- To analyze MH sensitivity

$$\Delta\chi^2_{MH} = \chi^2_{true}(\gamma \neq 0, \Delta m^2_{31} > 0) - \chi^2_{test}(\gamma = 0, \Delta m^2_{31} < 0)\,, \tag{12}$$

here we marginalized over θ_{23} and δ_{CP}.

We obtain significance of CPV and MH sensitivity using

$$\sigma_{CPV/MH} = \sqrt{\chi^2_{CPV/MH}}\,. \tag{13}$$

Table 3: True oscillation parameters and fit ranges have been considered in our analysis are taken from NuFIT [23].

Parameters	True values	Fit ranges
$\sin^2\theta_{12}$	0.304	Fixed
$\sin^2\theta_{13}$	0.0222	Fixed
$\sin^2\theta_{23}$	0.573	[0.405 : 0.620]
δ_{CP}	194°	[0 : 360°]
$\frac{\Delta m^2_{21}}{10^{-5}\ eV^2}$	7.42	Fixed
$\frac{\Delta m^2_{31}}{10^{-3}\ eV^2}$ (NH)	2.515	[2.431 : 2.599]
$\frac{\Delta m^2_{31}}{10^{-3}\ eV^2}$ (IH)	−2.498	[−2.584 : −2.413]

5 Results and discussion

In this section, we present our results for case-I and case-II (for other mentioned cases in table-1 please see ref. [11]). In each case we display $\nu_\mu \to \nu_e$, $\nu_\mu \to \nu_\mu$ and $\nu_\mu \to \nu_\tau$ oscillation channels. We illustrate the analytical behaviour of $P_{\mu e}$ in presence of γ_{jk}. However, for sensitivity analysis we consider relevant oscillation channels, such as ν_e appearance, ν_μ disappearance channels and corresponding antineutrinos channels. Considering event information from these channels we provide 90% and 3σ bounds on γ_{jk} parameters assuming no decoherence in nature (*true* value) and with decoherence in *test* hypothesis, as defined in eq. (10). Then we analyse CPV and MH sensitivity in the framework of decoherence present in nature and fitting the data with the standard model (SM). We assume 3σ value of γ_0 obtained from corresponding bounds in the *true* and follow the $\Delta\chi^2_{CPV/MH}$ definitions as mentioned in eqs. (11) and (12).

5.1 Case I : $\gamma_{21} = \gamma_{31} = \gamma_{32}$

In this case we assume all γ parameters are equal and non-zero. Considering this case, in fig. 1 we show ν_e-appearance (left), ν_μ-disappearance (middle) and ν_τ-appearance (right) probabilities for energy *power law* dependency on γ (eq. (8)) with $n = 0, \pm1, \pm2$ as mentioned in the legends. To calculate oscillation probabilities we choose the central values of oscillation parameters from table 3 and a representative value of $\gamma_{jk} = 2.3 \times 10^{-23}\ GeV$. Nevertheless, $\gamma_{jk} = 0$ leads to the standard model (SM) case. From fig. 1, we observe that all the channels are affected by the chosen set of γ parameters. Additionally, $n \geq 0$ show better variation w.r.t the SM scenario. It is noteworthy to mention that for $E_\nu \sim 10\, GeV$ a bump (dip) arises in the $P_{\mu e}$ ($P_{\mu\mu}$) channel in presence of decoherence effect. The origin of this bump/dip is illustrated in ref. [10, 11].

In fig. 2, we present sensitivity plots for case-I with 90 kW beam (upper row) and 450 kW (lower row) beam. In the left panel, we display upper bounds on γ with 90% (dashed line) and 3σ (dotted line) confidence level (CL) for *power law* dependencies $n = 0, \pm1, \pm2$. We calculate $\Delta\chi^2$ as per eq. (10) and listed the upper bounds in table-4 (90 kW) and table-5 (450 kW) with 90% and 3σ CL. It is noticeable that $n \geq 0$ provide stronger constraints on γ for both 90 kW and 450 kW beam as expected.

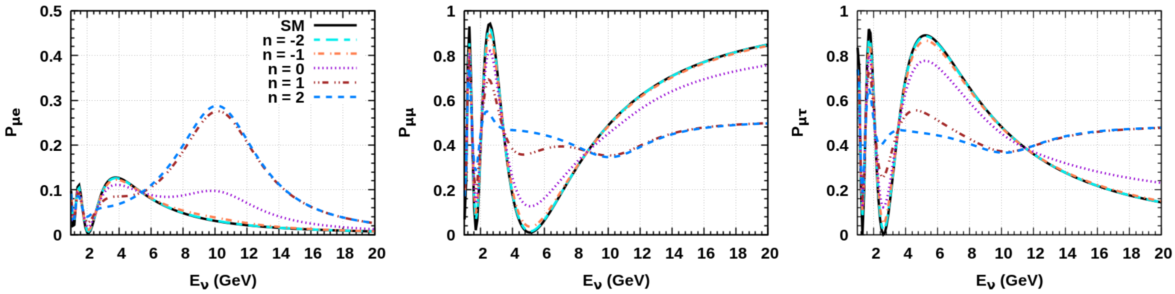

Figure 1: Oscillation probability as a function of neutrino energy for case-I. In the left, middle and right panel corresponding to ν_e appearance, ν_μ disappearance and ν_τ appearance channel respectively.

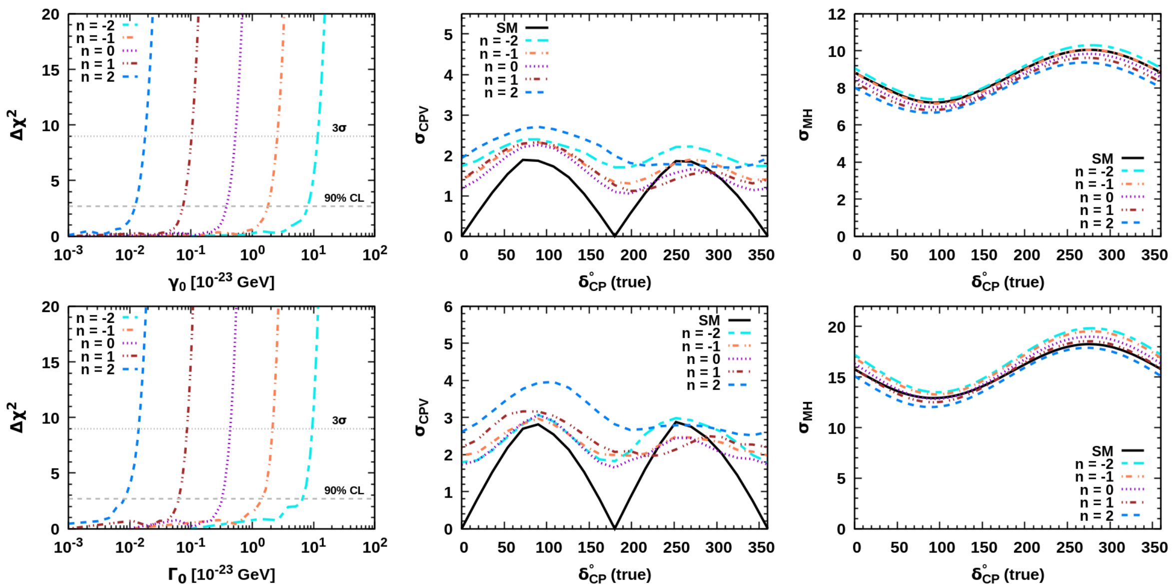

Figure 2: Sensitivity for case-I. Bounds on γ_0 in the left, CPV sensitivity in the middle and MH sensitivity in the right panel. Upper (lower) row represents the analysis considering 90 kW (450 kW) beam.

In the middle panel of fig. 2 we show CP-violation sensitivity (σ_{CPV}) as a function of *true* δ_{CP} considering decoherence exist in nature and fitting with the SM ($\gamma = 0$) paradigm. To obtain these plots with decoherence we take 3σ values of γ_0 in the *true* value (obtained in the corresponding left plot) and analyse accord with eqs. (11) and (13) . We observe that CPV sensitivities are effected significantly (w.r.t SM) in the presence of decoherence. Note that, in the presence of decoherence, conserving values of δ_{CP} ($= 0, \pm\pi$) are also show non-zero δ_{CP} with $\sim 2\sigma$ CL. This is a consequence of fake CP violation introduced by decoherence when the decoherence phenomenon exists in nature and we fit the data with SM.

In the right panel of fig. 2, we illustrate mass-hierarchy sensitivity (σ_{MH}) w.r.t δ_{CP} (*true*) considering NH as *true* and IH (inverted hierarchy) in *test*. We calculate the MH sensitivity for SM which is more than 5σ CL for all values of δ_{CP}(*true*) in both 90kW and 450kW beam. Then we calculate σ_{MH} by taking into account 3σ values of γ_0 (from tables-4 & 5) in the *true* value and *fitting* with the SM as in eqs. (12) & (13) for different n. We notice that MH sensitivity does not vary significantly w.r.t SM in presence of decoherence in both P2O and P2O-upgrade.

5.2 Case II: $\gamma_{21} = \gamma_{31},\ \gamma_{32} = 0$

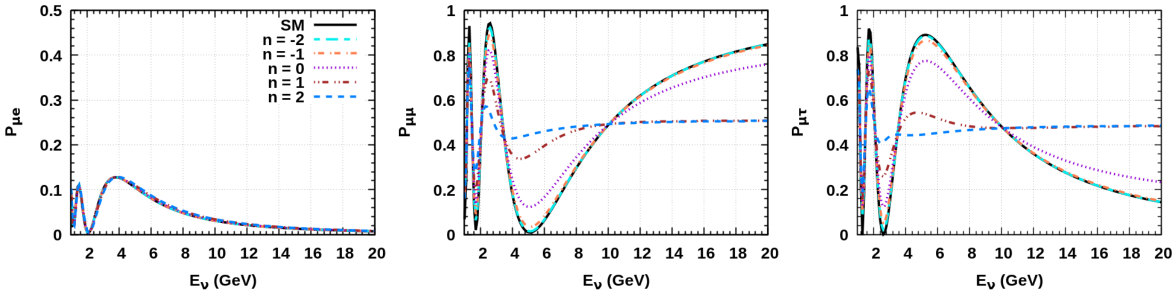

Figure 3: Oscillation probability as a function of neutrino energy for case-II. In the left, middle and right panel corresponding to ν_e appearance, ν_μ disappearance and ν_τ appearance channel respectively.

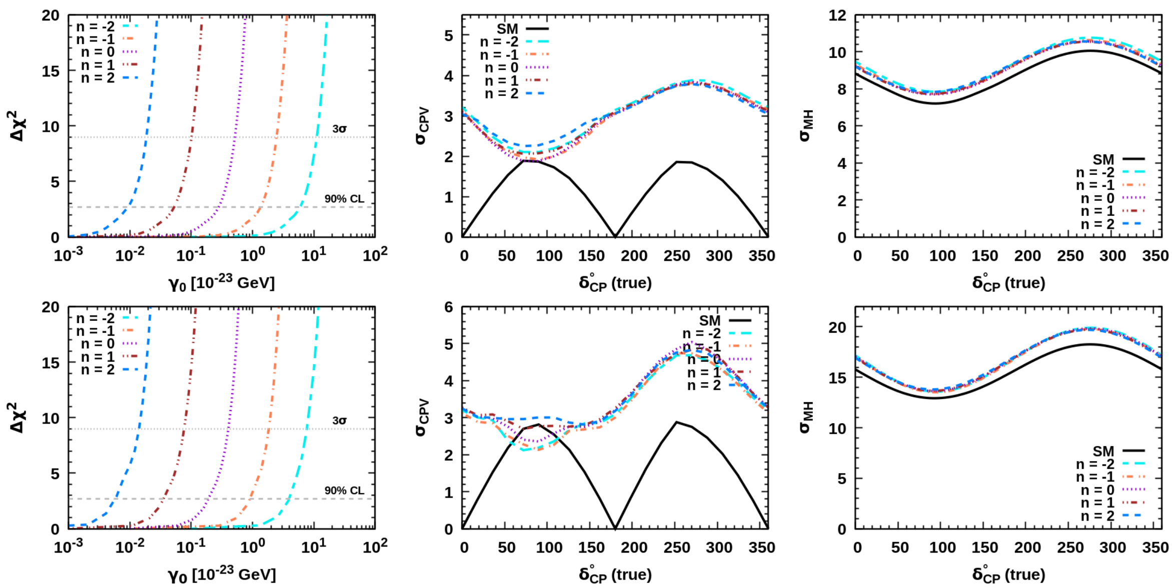

Figure 4: Sensitivity for case-II. Bounds on γ_0 in the left, CPV sensitivity in the middle and MH sensitivity in the right panel. Upper (lower) row represents the analysis considering 90 kW (450 kW) beam.

In this case we consider two of the γ parameters are non-zero and equal. We illustrate oscillation probability and sensitivity correspond to this case in fig. 3 and fig. 4. In fig. 3, we present oscillation probability corresponds to $\nu_\mu \to \nu_e$ (left), $\nu_\mu \to \nu_\mu$ (right) and $\nu_\mu \to \nu_\tau$ (right) channels. In each figure we have shown probability for SM and $n = 0, \pm 1, \pm 2$. Comparing with the SM, from the left plot we can see $P_{\mu e}$ is hardly affected (for explanation see ref. [11]) by the non-zero γ but $P_{\mu\mu}$ (middle) and $P_{\mu\tau}$ (right) are affected significantly.

In fig. 4, the left panel shows the upper bound on γ_0 and The middle (lower) panel represents CPV (MH) sensitivity for case-II (analysis procedure as discussed in the case-I). The upper and lower rows are the results for 90 kW and 450 kW proton beam at P2O. The upper bounds on γ_0, analysing this case for different power law dependencies, are listed in table-4 (90 kW) and table-5 (450 kW). From the middle panel we observe the conserving values of δ_{CP} are also show non-zero CPV. From the right panel we see that MH sensitivity do not vary significantly w.r.t SM for all power law and even if we increase the beam power.

Table 4: Bounds obtained in different cases for 90 kW beam power.

n	CL	Case-I $\gamma_{21} = \gamma_{31} = \gamma_{32}$	Case-II $\gamma_{21} = \gamma_{31}$	Case-III $\gamma_{21} = \gamma_{32}$	Case-IV $\gamma_{31} = \gamma_{32}$
$n = -2$	90%	8.06×10^{-23}	6.0×10^{-23}	1.008×10^{-22}	8.0×10^{-23}
	3σ	1.15×10^{-22}	1.11×10^{-22}	1.56×10^{-22}	1.15×10^{-22}
$n = -1$	90%	1.8×10^{-23}	1.36×10^{-23}	2.19×10^{-23}	1.75×10^{-23}
	3σ	2.55×10^{-23}	2.46×10^{-23}	3.37×10^{-23}	2.53×10^{-23}
$n = 0$	90%	3.76×10^{-24}	2.76×10^{-24}	4.26×10^{-24}	3.76×10^{-24}
	3σ	5.3×10^{-24}	5.18×10^{-24}	6.7×10^{-24}	5.23×10^{-24}
$n = 1$	90%	7.4×10^{-25}	5.4×10^{-25}	7.31×10^{-25}	7.3×10^{-25}
	3σ	1.04×10^{-24}	1.02×10^{-24}	1.23×10^{-24}	1.008×10^{-24}
$n = 2$	90%	1.24×10^{-25}	9.07×10^{-26}	1.007×10^{-25}	1.2×10^{-25}
	3σ	1.79×10^{-25}	1.87×10^{-25}	1.95×10^{-25}	1.74×10^{-25}

Table 5: Bounds obtained in different cases for 450 kW beam power.

n	CL	Case-I $\gamma_{21} = \gamma_{31} = \gamma_{32}$	Case-II $\gamma_{21} = \gamma_{31}$	Case-III $\gamma_{21} = \gamma_{32}$	Case-IV $\gamma_{31} = \gamma_{32}$
$n = -2$	90%	6.4×10^{-23}	3.9×10^{-23}	6.5×10^{-23}	6.4×10^{-23}
	3σ	9.0×10^{-23}	7.6×10^{-23}	1.1×10^{-22}	9.3×10^{-23}
$n = -1$	90%	1.4×10^{-23}	8.5×10^{-24}	1.5×10^{-23}	1.46×10^{-23}
	3σ	2.1×10^{-23}	1.75×10^{-23}	2.5×10^{-23}	2.0×10^{-23}
$n = 0$	90%	3.1×10^{-24}	1.89×10^{-24}	2.5×10^{-24}	3.1×10^{-24}
	3σ	4.2×10^{-24}	4.0×10^{-24}	5.0×10^{-24}	4.7×10^{-24}
$n = 1$	90%	6.2×10^{-25}	3.6×10^{-25}	4.2×10^{-25}	6.3×10^{-25}
	3σ	8.5×10^{-25}	7.7×10^{-25}	8.5×10^{-25}	8.1×10^{-25}
$n = 2$	90%	7.8×10^{-26}	5.87×10^{-26}	6.0×10^{-26}	7.5×10^{-26}
	3σ	1.5×10^{-25}	1.4×10^{-25}	1.1×10^{-25}	1.3×10^{-25}

However, in this proceeding we have described first two cases mentioned in the table-1. Nevertheless, in table-4 and table-5 we have presented expected upper bounds on decoherence parameters for all four cases. We refer [11] for complete description of all four cases.

6 Conclusions

In a model-independent approach we obtain the upper bounds on γ considering *power law* dependency ($\gamma \propto E^n$, $n = 0, \pm1, \pm2$) for future P2O experiment. We observe that, $n \geq 0$ show comparatively better constraints on γ parameter for both P2O and upgrade-P2O. Specifically, for case-II ($\Gamma_{21} = \Gamma_{31}$, $\Gamma_{32} = 0$) poses strong constraints for $n = 0$ on $\Gamma \leq 2.76 \times 10^{-24}$ GeV for P2O and $\Gamma \leq 1.89{\times}10^{-24}$ GeV for P2O-upgrade, which are stronger than the upper bounds obtained in ref. [8] ($n = 0$ column in table 3) and competitive with the bounds obtained in ref. [7] from IceCube data.

We also present CPV and MH sensitivity in presence of decoherence. Considering non-zero decoherence in the *true* and no decoherence hypothesis in the *test*, we notice that, CP conserving values ($\delta_{CP} = 0, \pm\pi$) are also give non-zero δ_{CP}. Which indicates decoherence could introduce a fake CP phase and mislead the CP-violation. However, using similar hypothesis we observe marginal impact of decoherence on MH sensitivity.

References

[1] E. Lisi, A. Marrone, D. Montanino, Probing possible decoherence effects in atmospheric neutrino oscillations, Phys. Rev. Lett. **85**, 1166 (2000), `hep-ph/0002053`. 10.1103/PhysRevLett.85.1166

[2] G.L. Fogli, E. Lisi, A. Marrone, D. Montanino, A. Palazzo, Probing non-standard decoherence effects with solar and KamLAND neutrinos, Phys. Rev. D **76**, 033006 (2007), `0704.2568`. 10.1103/PhysRevD.76.033006

[3] G. Balieiro Gomes, M.M. Guzzo, P.C. de Holanda, R.L.N. Oliveira, Parameter Limits for Neutrino Oscillation with Decoherence in KamLAND, Phys. Rev. D **95**, 113005 (2017), `1603.04126`. 10.1103/PhysRevD.95.113005

[4] A.L.G. Gomes, R.A. Gomes, O.L.G. Peres, Quantum decoherence and relaxation in long-baseline neutrino data, JHEP **10**, 035 (2023), `2001.09250`. 10.1007/JHEP10(2023)035

[5] J.A.B. Coelho, W.A. Mann, S.S. Bashar, Nonmaximal θ_{23} mixing at NOvA from neutrino decoherence, Phys. Rev. Lett. **118**, 221801 (2017), `1702.04738`. 10.1103/PhysRevLett.118.221801

[6] P. Coloma, J. Lopez-Pavon, I. Martinez-Soler, H. Nunokawa, Decoherence in Neutrino Propagation Through Matter, and Bounds from IceCube/DeepCore, Eur. Phys. J. C **78**, 614 (2018), `1803.04438`. 10.1140/epjc/s10052-018-6092-6

[7] R. Abbasi et al. (IceCube), Searching for Decoherence from Quantum Gravity at the IceCube South Pole Neutrino Observatory, Nature Physics (2024), `2308.00105`. 10.1038/s41567-024-02436-w

[8] V. De Romeri, C. Giunti, T. Stuttard, C.A. Ternes, Neutrino oscillation bounds on quantum decoherence, JHEP **09**, 097 (2023), `2306.14699`. 10.1007/JHEP09(2023)097

[9] J.A. Carpio, E. Massoni, A.M. Gago, Testing quantum decoherence at DUNE, Phys. Rev. D **100**, 015035 (2019), `1811.07923`. 10.1103/PhysRevD.100.015035

[10] G. Balieiro Gomes, D.V. Forero, M.M. Guzzo, P.C. De Holanda, R.L.N. Oliveira, Quantum Decoherence Effects in Neutrino Oscillations at DUNE, Phys. Rev. D **100**, 055023 (2019), `1805.09818`. 10.1103/PhysRevD.100.055023

[11] C. Bera, K.N. Deepthi, Study of quantum decoherence at Protvino to ORCA experiment, arXiv (2024), `2405.03286`. https://doi.org/10.48550/arXiv.2405.03286

[12] G. Lindblad, On the Generators of Quantum Dynamical Semigroups, Commun. Math. Phys. **48**, 119 (1976). 10.1007/BF01608499

[13] V. Gorini, A. Kossakowski, E.C.G. Sudarshan, Completely Positive Dynamical Semigroups of N Level Systems, J. Math. Phys. **17**, 821 (1976). 10.1063/1.522979

[14] V. Gorini, A. Frigerio, M. Verri, A. Kossakowski, E.C.G. Sudarshan, Properties of Quantum Markovian Master Equations, Rept. Math. Phys. **13**, 149 (1978). 10.1016/0034-4877(78)90050-2

[15] T. Banks, L. Susskind, M.E. Peskin, Difficulties for the Evolution of Pure States Into Mixed States, Nucl. Phys. B **244**, 125 (1984). 10.1016/0550-3213(84)90184-6

[16] F. Benatti, H. Narnhofer, ENTROPY BEHAVIOR UNDER COMPLETELY POSITIVE MAPS, Lett. Math. Phys. **15**, 325 (1988). 10.1007/BF00419590

[17] Y. Farzan, T. Schwetz, A.Y. Smirnov, Reconciling results of LSND, MiniBooNE and other experiments with soft decoherence, JHEP **07**, 067 (2008), 0805.2098. 10.1088/1126-6708/2008/07/067

[18] P.B. Denton, S.J. Parke, Addendum to "Compact perturbative expressions for neutrino oscillations in matter" (2018), [Addendum: JHEP 06, 109 (2018)], 1801.06514. 10.1007/JHEP06(2018)109

[19] P. Huber, M. Lindner, W. Winter, Simulation of long-baseline neutrino oscillation experiments with GLoBES (General Long Baseline Experiment Simulator), Comput. Phys. Commun. **167**, 195 (2005), hep-ph/0407333. 10.1016/j.cpc.2005.01.003

[20] P. Huber, J. Kopp, M. Lindner, M. Rolinec, W. Winter, New features in the simulation of neutrino oscillation experiments with GLoBES 3.0: General Long Baseline Experiment Simulator, Comput. Phys. Commun. **177**, 432 (2007), hep-ph/0701187. 10.1016/j.cpc.2007.05.004

[21] A.V. Akindinov et al., Letter of Interest for a Neutrino Beam from Protvino to KM3NeT/ORCA, Eur. Phys. J. C **79**, 758 (2019), 1902.06083. 10.1140/epjc/s10052-019-7259-5

[22] S. Adrian-Martinez et al. (KM3Net), Letter of intent for KM3NeT 2.0, J. Phys. G **43**, 084001 (2016), 1601.07459. 10.1088/0954-3899/43/8/084001

[23] I. Esteban, M.C. Gonzalez-Garcia, M. Maltoni, T. Schwetz, A. Zhou, The fate of hints: updated global analysis of three-flavor neutrino oscillations, JHEP **09**, 178 (2020), 2007.14792. 10.1007/JHEP09(2020)178

[24] G.L. Fogli, E. Lisi, A. Marrone, D. Montanino, A. Palazzo, Getting the most from the statistical analysis of solar neutrino oscillations, Phys. Rev. D **66**, 053010 (2002), hep-ph/0206162. 10.1103/PhysRevD.66.053010

[25] P. Huber, M. Lindner, W. Winter, Superbeams versus neutrino factories, Nucl. Phys. B **645**, 3 (2002), hep-ph/0204352. 10.1016/S0550-3213(02)00825-8

https://doi.org/10.1051/epjconf/202431202011

edp sciences

Web of Conferences

License Agreement

In submitting an article to *Web of Conferences,* I grant EDP Sciences a license to publish the article, and identify EDP Sciences as the original publisher. I certify to the Publisher that:

1. I am authorized by my co-authors to enter into these arrangements.

2. I warrant, on behalf of myself and my co-authors, that:
   - the document is original, has not been formally published in any other journal, is not under consideration by any other journal. If parts from copyrighted works owned by third parties are included (included figures, tables etc.), written permission is obtained from the copyright owners for all uses as set forth in the Journal's Instructions for Authors, and credit to the sources is shown in the Manuscript. This permission is obtained for reproduction in a publication in Open Access with a CC-by 4.0 License;
   - I am/we are the sole author(s) of the article and have full authority to enter into this agreement and in granting rights to the Publisher that are not in breach of any other obligation.
   - the document contains nothing that is unlawful, libelous, or which would, if published, constitute a breach of contract or of confidence or of commitment given to secrecy;
   - I/we have taken due care to ensure the integrity of the article. To my/our – and currently accepted scientific – knowledge all statements contained in it purporting to be facts are true and any formula or instruction contained in the article will not, if followed accurately, cause any injury, illness or damage to the user.

3. I agree to the Creative Commons Attribution License (https://creativecommons.org/licenses/by/4.0/).

Title of the conference

22nd Conference on Flavour Physics and CP violation (FPCP2024)

Title of the article

QUANTUM DECOHERENCE AND CP VIOLATION AT PROTVINO TO ORCA

Author(s)

CHINMAY BERA

DEEPTHI K N

Author's signature

Chinmay (Chinmay Bera)

Deepthi (Deepthi K N)

Date: 29-7-2024